

Ice Skating Motion Using Feedforward Control System by Model of Humanoid Robot

Zeyi Zhang¹, Daiji Izawa¹, Xiang Li¹, Takayuki Matsuno¹, Mamoru Minami¹

¹Okayama University, Japan
(Tel:81-86-251-8233, Fax:81-86-251-8233)
¹peiw4znm@s.okayama-u.ac.jp

Abstract: The research of humanoid is widely discussed whether by simulations or real machines. To bipedal walking, inverted pendulum has been used frequently for making a stable controller that enables researchers to realize stable gait through well-known control strategy. In our research, a model of humanoid robot including slipping, bumping, surface-contacting and point-contacting of foot is discussed, and its dynamical equation is derived by Newton-Euler method. Our research purpose aims to create a control system by utilize slip and stop slip using the model. In this paper, the ice skating, which is a kind of typical utilize slip motion will be discussed. And a new feedforward control method was prepared for realize this motion. Also some discussion from the viewpoint of step cycle and slipping distance during the ice skating motion will be introduced.

Keywords: Humanoid, slipping, Bipedal, Dynamical, Newton-Euler Method

1 INTRODUCTION

Human beings have acquired an ability of stable bipedal walking in evolving repetitions so far. From a view point of making a stable controller for the bipedal walking based on knowledge of conventional control theory, it looks not easy because of the dynamics with high nonlinearity and coupled interactions between links of humanoid with high dimensions. Avoiding complications in dealing directly with true dynamics without approximation, an inverted pendulum model has been used frequently for making a stable controller[1]-[3], simplifying the calculations to determine input torque. Further, linear approximation having the humanoid represented by simple inverted pendulum enables researchers to realize stable gait through well-known control strategy[4]-[6].

Our research has begun from the view point as aiming to describe gait's dynamics as correctly as possible, including point-contacting state of foot and toe, slipping of the foot and bumping [7] [8]. Meanwhile, landing of the heel or the toe of lifting leg in the air to the ground makes a geometrical contact. Based on [10]. The dynamics of humanoid can be modeled as a serial-link manipulator including constraint motion and slipping motion by using the Extended Newton-Euler(NE) Method[11]. In this research that based on [12], a walking model of humanoid robot including slipping, bumping, surface contacting and point-contacting of foot was discussed.

In this paper, the slipping of the foot of humanoid robot when the friction coefficient is small (on the ice, snow, or wet road) has been modeled to discuss walking motion and slipping behavior. The new model of humanoid robot and gait models have been proposed. And gait models include

both slip and stick will be verified through the simulation experiments.

2 DYNAMICAL WALKING MODEL

2.1 Humanoid Model

We discuss a bipedal robot whose definition is depicted in Fig.1. Table 1 lists length l_i [m], mass m_i [kg] of links and coefficient of joints' viscous friction d_i [N·m·s/rad], which are decided based on [13]. This model is simulated as a serial-link manipulator having ramifications and represents rigid whole body—feet including toe, torso, arms and so on—by 17 DoF. Though motion of legs is restricted in sagittal plane, it generates varieties of walking gait sequences since the robot has flat-sole feet and kicking torque on ankle. In this paper, one foot including link-1 is defined as “supporting-leg” and another foot including link-7 is defined as “free-leg” (“contacting-leg” when the free-leg contacts with floor) according to the walking state.

In this paper, we derive the equation of motion following by NE formulation. So we consider the structure of the supporting leg with two situations. When the supporting leg is constituted of rotating joint, we first have to calculate relations of positions, velocities and accelerations between links as forward kinetics procedures from bottom link to top link. Serial link's angular velocity ${}^i\omega_i$, angular acceleration ${}^i\dot{\omega}_i$, acceleration of the origin ${}^i\ddot{p}_i$ and acceleration of the center of mass ${}^i\ddot{s}_i$ based on Σ_i fixed at i -th link are obtained as

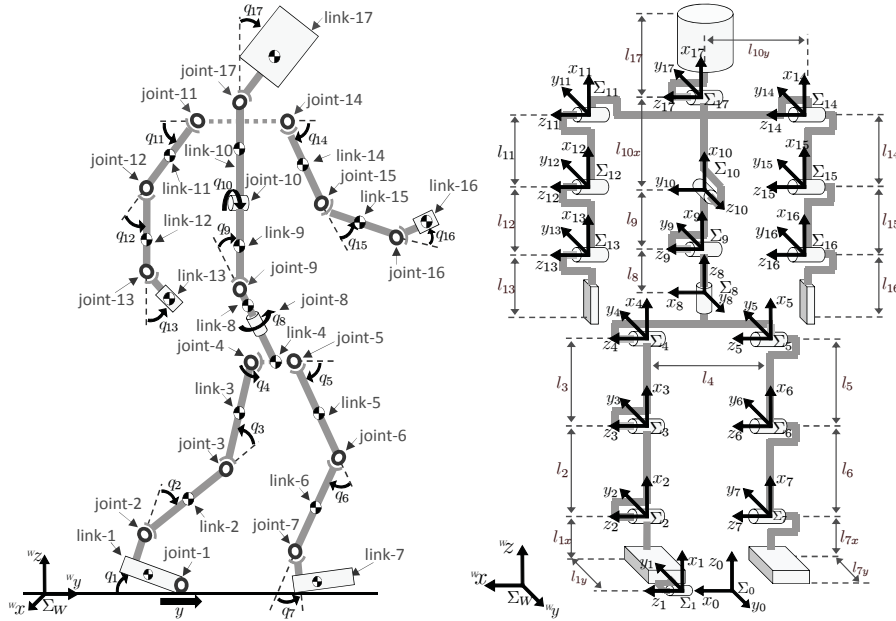


Table 1. Physical parameters

Link	l_i	m_i	d_i
Head	0.24	4.5	0.5
Upper body	0.41	21.5	10.0
Middle body	0.1	2.0	10.0
Lower body	0.1	2.0	10.0
Upper arm	0.31	2.3	0.03
Lower arm	0.24	1.4	1.0
Hand	0.18	0.4	2.0
Waist	0.27	2.0	10.0
Upper leg	0.38	7.3	10.0
Lower leg	0.40	3.4	10.0
Foot	0.07	1.3	10.0
Total weight [kg]	—	64.2	—
Total height [m]	1.7	—	—

Fig. 1. Definition of humanoid's link, joint and coordinate system

follows.

$${}^i\omega_i = {}^{i-1}R_i^T {}^{i-1}\omega_{i-1} + e_{z_i} \dot{q}_i \quad (1)$$

$${}^i\dot{\omega}_i = {}^{i-1}R_i^T {}^{i-1}\dot{\omega}_{i-1} + e_{z_i} \ddot{q}_i + {}^i\omega_i \times (e_{z_i} \dot{q}_i) \quad (2)$$

$${}^i\ddot{p}_i = {}^{i-1}R_i^T \left\{ {}^{i-1}\ddot{p}_{i-1} + {}^{i-1}\dot{\omega}_{i-1} \times {}^{i-1}\hat{p}_i + {}^{i-1}\omega_{i-1} \times ({}^{i-1}\omega_{i-1} \times {}^{i-1}\hat{p}_i) \right\} \quad (3)$$

$${}^i\ddot{s}_i = {}^i\ddot{p}_i + {}^i\dot{\omega}_i \times {}^i\hat{s}_i + {}^i\omega_i \times ({}^i\omega_i \times {}^i\hat{s}_i) \quad (4)$$

Then if the supporting leg is constituted of prismatic form object, that describes slipping motion along ${}^w y$ direction in Fig.1. The equations is switched as the following.

$${}^i\omega_i = {}^{i-1}R_i^T {}^{i-1}\omega_{i-1} \quad (5)$$

$${}^i\dot{\omega}_i = {}^{i-1}R_i^T {}^{i-1}\dot{\omega}_{i-1} \quad (6)$$

$${}^i\ddot{p}_i = {}^{i-1}R_i^T \left\{ {}^{i-1}\ddot{p}_{i-1} + {}^{i-1}\dot{\omega}_{i-1} \times {}^{i-1}\hat{p}_i + {}^{i-1}\omega_{i-1} \times ({}^{i-1}\omega_{i-1} \times {}^{i-1}\hat{p}_i) \right\} + 2({}^{i-1}R_i^T {}^{i-1}\omega_{i-1}) \times (e_{z_i} \dot{q}_i) + e_{z_i} \ddot{q}_i \quad (7)$$

$${}^i\ddot{s}_i = {}^i\ddot{p}_i + {}^i\dot{\omega}_i \times {}^i\hat{s}_i + {}^i\omega_i \times ({}^i\omega_i \times {}^i\hat{s}_i) \quad (8)$$

Here, ${}^{i-1}R_i$ means orientation matrix, ${}^{i-1}\hat{p}_i$ represents position vector from the origin of $(i-1)$ -th link to the one of i -th, ${}^i\hat{s}_i$ is defined as gravity center position of i -th link and e_{z_i} is unit vector that shows rotational axis of i -th link.

After the above forward kinetic has been calculated, contrarily inverse dynamical calculation from top to base link are calculated.

Finally, we get motion equation with one leg standing as:

$$M(q)\ddot{q} + h(q, \dot{q}) + g(q) + D\dot{q} = \tau, \quad (9)$$

Here, $\tau = [f_1, \tau_1, \tau_2, \dots, \tau_{17}]$ is input torque, $M(q)$ is inertia matrix, both of $h(q, \dot{q})$ and $g(q)$ are vectors which indicate Coriolis force, centrifugal force and gravity. When the supporting leg is slipping, the $D = \text{diag}[\mu_k, d_1, d_2, \dots, d_{17}]$ is a matrix which means coefficients between foot and ground, and $q = [y_0, q_1, q_2, \dots, q_{17}]^T$ means the relative position between foot and ground and that of joints. The vector q changes according to the state of the supporting foot as shown in Fig. 2.

2.2 Constraint Conditions for free-leg Model

When making free-leg contact with ground, the free leg appears with the position or angle to the ground being constrained. Also, when velocity of free leg's in traveling direction becomes less than 0.01[m/s], the free leg is constrained in acceleration by the static friction. The constraints of foot's z-axis position, heel's rotation (c) and foot's y-axis position on floating foot are defined as C_1 , C_2 and C_3 respectively, these constraints can be written as follow, where $r(q)$ means heel

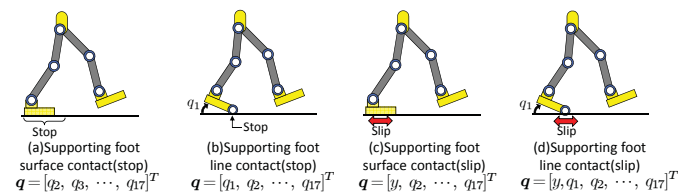


Fig. 2. Ground state of the supporting foot

position of free leg or toe position of it in Σ_W .

$$C(\mathbf{r}(\mathbf{q})) = \begin{bmatrix} C_1(\mathbf{r}(\mathbf{q})) \\ C_2(\mathbf{r}(\mathbf{q})) \\ C_3(\mathbf{r}(\mathbf{q})) \end{bmatrix} = \mathbf{0} \quad (10)$$

Then, equation of motion with external force f_{nz} , friction force f_t , external torque τ_n and external force f_{ny} corresponding to C_1 , C_2 and C_3 can be derived as:

$$\begin{aligned} M(\mathbf{q})\ddot{\mathbf{q}} + \mathbf{h}(\mathbf{q}, \dot{\mathbf{q}}) + \mathbf{g}(\mathbf{q}) + D\dot{\mathbf{q}} \\ = \boldsymbol{\tau} + \mathbf{j}_{cz}^T f_{nz} - \mathbf{j}_t^T f_t + \mathbf{j}_r^T \tau_n + \mathbf{j}_{cy}^T f_{ny} \end{aligned} \quad (11)$$

where \mathbf{j}_{cz} , \mathbf{j}_t , \mathbf{j}_r and \mathbf{j}_{cy} are defined as:

$$\begin{aligned} \mathbf{j}_{cz}^T &= \left(\frac{\partial \mathbf{r}}{\partial \mathbf{q}^T} \right)^T \left(\frac{\partial C_1}{\partial \mathbf{q}^T} / \left\| \frac{\partial C_1}{\partial \mathbf{r}^T} \right\| \right), \quad \mathbf{j}_t^T = \left(\frac{\partial \mathbf{r}}{\partial \mathbf{q}^T} \right)^T \frac{\dot{\mathbf{r}}}{\|\dot{\mathbf{r}}\|}, \\ \mathbf{j}_r^T &= \frac{\partial C_2}{\partial \mathbf{r}^T} / \left\| \frac{\partial C_2}{\partial \mathbf{r}^T} \right\|, \quad \mathbf{j}_{cy}^T = \left(\frac{\partial \mathbf{r}}{\partial \mathbf{q}^T} \right)^T \left(\frac{\partial C_3}{\partial \mathbf{q}^T} / \left\| \frac{\partial C_3}{\partial \mathbf{q}^T} \right\| \right) \end{aligned} \quad (12)$$

By differentiating equation (14) second-order by time t and simultaneous with equation (15), the following dynamics is obtained

$$\begin{aligned} \begin{bmatrix} M(\mathbf{q}) & -(\mathbf{j}_{cz}^T - \mathbf{j}_t^T K) & -\mathbf{j}_r^T & -\mathbf{j}_{cy}^T \\ \partial C_1 / \partial \mathbf{q}^T & 0 & 0 & 0 \\ \partial C_2 / \partial \mathbf{q}^T & 0 & 0 & 0 \\ \partial C_3 / \partial \mathbf{q}^T & 0 & 0 & 0 \end{bmatrix} \begin{bmatrix} \ddot{\mathbf{q}} \\ f_{nz} \\ \tau_n \\ f_{ny} \end{bmatrix} \\ = \begin{bmatrix} \boldsymbol{\tau} - \mathbf{h}(\mathbf{q}, \dot{\mathbf{q}}) - \mathbf{g}(\mathbf{q}) - D\dot{\mathbf{q}} \\ -\dot{\mathbf{q}}^T \left\{ \frac{\partial}{\partial \mathbf{q}} \left(\frac{\partial C_1}{\partial \mathbf{q}^T} \right) \right\} \dot{\mathbf{q}} \\ -\dot{\mathbf{q}}^T \left\{ \frac{\partial}{\partial \mathbf{q}} \left(\frac{\partial C_2}{\partial \mathbf{q}^T} \right) \right\} \dot{\mathbf{q}} \\ -\dot{\mathbf{q}}^T \left\{ \frac{\partial}{\partial \mathbf{q}} \left(\frac{\partial C_3}{\partial \mathbf{q}^T} \right) \right\} \dot{\mathbf{q}} \end{bmatrix} \end{aligned} \quad (13)$$

3 GAIT MODELS

3.1 Extension of dynamics

The contact state of each legs is determined by the solution of the dynamics in Eq.(17), which is shown in the previous section. This state variously changes while walking. So we have prepared 20 kinds of gait models according to the states and have realized walking by the transition of gaits state. All of the walking dynamical models include the constrain conditions as shown in Table 2.

3.2 Transition of gait state

Based on each gait model created in the previous section, the gait transition diagram shown in Fig.3 was created. The number in the upper left of each gait model in the figure corresponds to Table.2 shown in the previous section. Regarding the pathway of the gait transition, the equation of motion is determined by the walking motion of the humanoid.

Table 2. Possible states for humanoid's walking

State number	State variables and constraining force and torque (Lagrange Multiplier)	Constraints (reference)
1	$\mathbf{q} = [q_2, q_3, \dots, q_{17}]^T$	Nothing
2	$\mathbf{q} = [q_1, q_2, \dots, q_{17}]^T$	Nothing
3	$\mathbf{q} = [y_0, q_2, \dots, q_{17}]^T$	Nothing
4	$\mathbf{q} = [y_0, q_1, \dots, q_{17}]^T$	Nothing
5	$\mathbf{q} = [q_2, q_3, \dots, q_{17}]^T, f_{nz}$	$C_{hz} = 0$
6	$\mathbf{q} = [q_1, q_2, \dots, q_{17}]^T, f_{nz}$	$C_{hz} = 0$
7	$\mathbf{q} = [y_0, q_2, q_3, \dots, q_{17}]^T, f_{nz}$	$C_{hz} = 0$
8	$\mathbf{q} = [y_0, q_1, q_2, q_3, \dots, q_{17}]^T, f_{nz}$	$C_{hz} = 0$
9	$\mathbf{q} = [q_2, q_3, \dots, q_{17}]^T, f_{nz}, f_{ny}$	$C_{hz}, C_{hy} = 0$
10	$\mathbf{q} = [q_1, q_2, \dots, q_{17}]^T, f_{nz}, f_{ny}$	$C_{hz}, C_{hy} = 0$
11	$\mathbf{q} = [y_0, q_2, q_3, \dots, q_{17}]^T, f_{nz}, f_{ny}$	$C_{hz}, C_{hy} = 0$
12	$\mathbf{q} = [y_0, q_1, q_2, q_3, \dots, q_{17}]^T, f_{nz}, f_{ny}$	$C_{hz}, C_{hy} = 0$
13	$\mathbf{q} = [q_2, q_3, \dots, q_{17}]^T, f_{nz}, \tau_n$	$C_{hz}, C_{fr} = 0$
14	$\mathbf{q} = [q_1, q_2, \dots, q_{17}]^T, f_{nz}, \tau_n$	$C_{hz}, C_{fr} = 0$
15	$\mathbf{q} = [y_0, q_2, q_3, \dots, q_{17}]^T, f_{nz}, \tau_n$	$C_{hz}, C_{fr} = 0$
16	$\mathbf{q} = [y_0, q_1, q_2, q_3, \dots, q_{17}]^T, f_{nz}, \tau_n$	$C_{hz}, C_{fr} = 0$
17	$\mathbf{q} = [q_2, q_3, \dots, q_{17}]^T, f_{ny}, f_{nz}, \tau_n$	$C_{hz}, C_{hy}, C_{fr} = 0$
18	$\mathbf{q} = [q_1, q_2, \dots, q_{17}]^T, f_{ny}, f_{nz}, \tau_n$	$C_{hz}, C_{hy}, C_{fr} = 0$
19	$\mathbf{q} = [y_0, q_2, q_3, \dots, q_{17}]^T, f_{ny}, f_{nz}, \tau_n$	$C_{hz}, C_{hy}, C_{fr} = 0$
20	$\mathbf{q} = [y_0, q_1, q_2, q_3, \dots, q_{17}]^T, f_{ny}, f_{nz}, \tau_n$	$C_{hz}, C_{hy}, C_{fr} = 0$

4 SIMULATION (ICE SKATING WALKING)

4.1 Coefficient of friction

The movement aimed in this paper is the motion of ice skating using the slip. As it is shown in Fig.1, the direction of walking is defined as the direction of positive y-axis. When proceeding to progressive walking, the friction coefficient between the foot and the ground is set to 0.2. However, in order to obtain acceleration force in the direction of travel by kicking out of the toe, the friction coefficient is set to 0.9 when a force acts in the opposite direction to the progressive walking. Similar to the principle of skates.

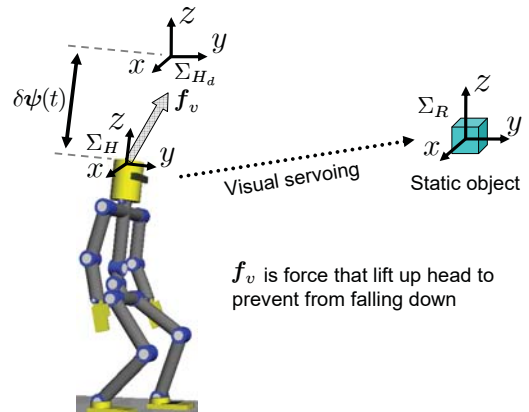


Fig. 4. Concept of Visual-Lifting Approach

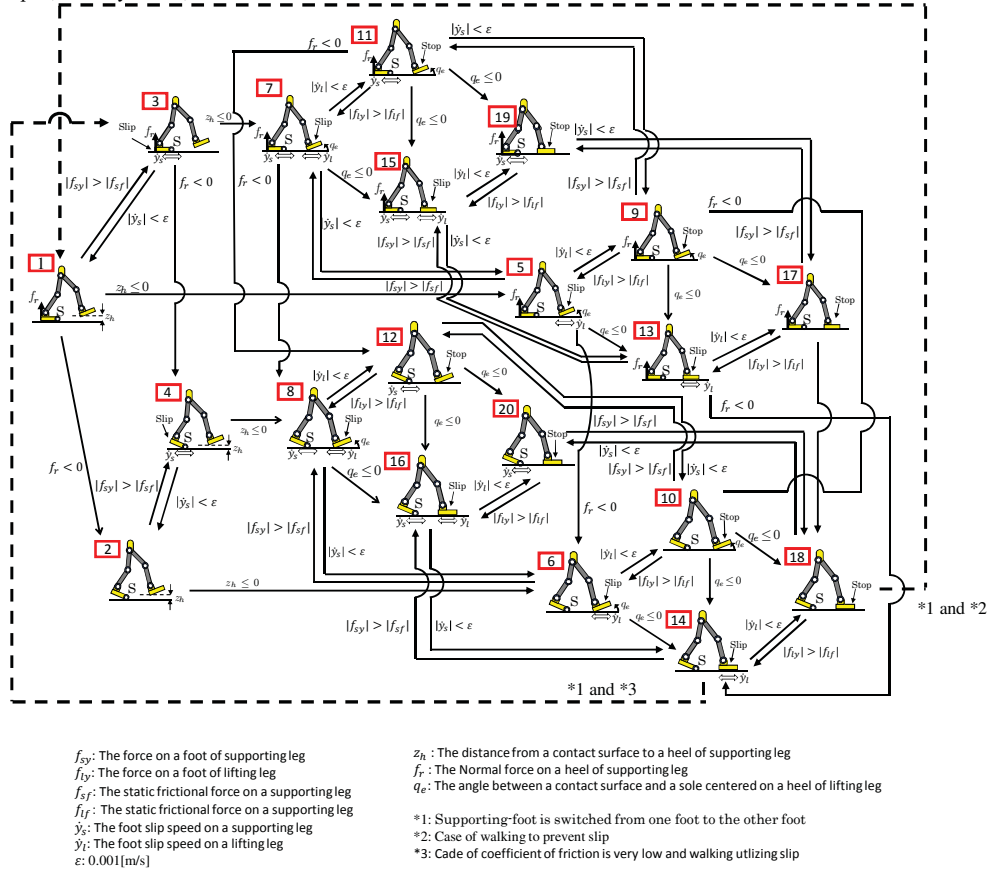


Fig. 3. Translation of bipedal walking

4.2 Input torque

4.2.1 Visual-Lifting Approach

This section proposes a visual-lifting feedback to improve biped standing/walking stability as shown in Fig.4. We apply a model-based matching method to evaluate posture of a static target object described by $\psi(t)$ representing the robot's head based on Σ_H . The relatively desired posture of Σ_R (coordinate of reference target object) and Σ_H is predefined by Homogeneous Transformation as ${}^H T_R$. The difference of the desired head posture Σ_{H_d} and the current posture Σ_H is defined as ${}^H T_{H_d}$, it can be described by:

$${}^H T_{H_d}(\psi_d(t), \psi(t)) = {}^H T_R(\psi(t)) \cdot {}^{H_d} T_R^{-1}(\psi_d(t)), \quad (14)$$

where ${}^H T_R$ is calculated by $\psi(t)$. $\psi(t)$ can be measured by on-line visual posture evaluation. However, we assume that this parameter is set directly. Here, the force is considered to be directly proportional to $\delta\psi(t)$, which is exerted on the head to minimize $\delta\psi(t) (= \psi_d(t) - \psi(t))$ calculated from ${}^H T_{H_d}$. The deviation of the robot's head posture is caused by gravity force and the influence of walking dynamics. The joint torque $\tau_h(t)$ lifting the robot's head is donated:

$$\tau_h(t) = J_h(q)^T K_p \delta\psi(t), \quad (15)$$

where $J_h(q)$ is Jacobian matrix of the head posture against joint angles including $q_1, q_2, q_3, q_4, q_8, q_9, q_{10}, q_{17}$, and K_p

is proportional gain like impedance control. We apply this input to stop falling down caused by gravity or dangerous slipping gaits happened unpredictably during walking progress. We stress that the input torque for non-noneconomic joint such as joint-1, τ_{h_1} in $\tau_h(t)$ in (15) is zero for its free joint. $\delta\psi(t)$ can show the deviation of the humanoid's position and orientation, however, only position is discussed in this study.

4.2.2 Foot and Body Motion Generator

Besides $\tau_h(t)$, in order to make the floating-foot and supporting-foot step forward, added input torques $\tau_i(t) = [\tau_1, \tau_2, \tau_3, 0, \tau_5, 0, \dots, 0]^T$ are used. Here, $\tau_i(t)$ and is seen as feed-forward input torques. Here, t_0 means the time that supporting-foot and contacting-foot are switched. t_1 means the time that state 3 trans to state 7. t_2 means the time that state 7 trans to state 16. The elements $\tau_t(t)$ are shown below:

$$\tau_1 = -100 \cos(2\pi(t_n - t_2)/2) \quad (\text{State} = 14 \text{ or } 16) \quad (16)$$

$$\tau_2 = \begin{cases} -205 \cos(2\pi(t_n - t_1)/2) & (\text{State} = 7) \\ -75 \cos(2\pi(t_n - t_2)/2) & (\text{State} = 14 \text{ or } 16) \end{cases} \quad (17)$$

$$\tau_3 = -50 \cos(2\pi(t_n - t_1)/2) \quad (\text{State} = 7) \quad (18)$$

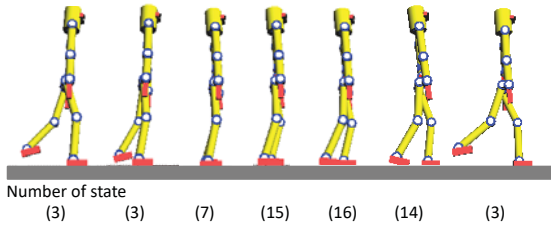


Fig. 5. Screen-shot while ice skating motion

$$\tau_5 = \begin{cases} 50 \cos(2\pi(t_n - t_0)/2) & (State = 3) \\ 100 \cos(2\pi(t_n - t_1)/2) & (State = 7) \\ 30 & (State = 116) \end{cases} \quad (19)$$

In addition to these, the following torque is given as an auxiliary input in order to keep the free leg heel at a fixed angle.

$$\tau_6 = 20 \quad (State = 3) \quad (20)$$

$$\tau_7 = \begin{cases} 50 & (State = 3, q_E < 0.25) \\ -30 & (State = 3, q_E \geq 0.25) \\ 40 & (State = 7, q_E > 0) \\ 0 & (State = 7, q_E \leq 0.25) \end{cases} \quad (21)$$

Here, q_E is the angle of the free leg relative to the ground.

4.3 Simulation result

Simulation was conducted based on the experimental conditions shown in the previous section. The simulation is stopped at the time of 100 steps of the humanoid model. Screenshots during simulation are shown in Fig. 5. Numbers in the figure indicate the gait number, which reflects the period from the start of the simulation to the start of the next step. As a result, the motion of the ice skating which was the motion using the slip was realized. As a method of gait transition, according to Fig.3, gait transitions that $3 \rightarrow 7 \rightarrow 15 \rightarrow 16 \rightarrow 14 \rightarrow 3$ is set. Fig.6 shows the Position of free-feet (joint-7) in z-axis in one step. Slide distance for each step are shown in Fig.7. Fig.8 shows the walking cycle for each step up to 100 steps.

4.4 Spontaneous arm swing

To cause swing of the arm, an input torque of yaw angle (joint - 8) is added. Fig.8-9 show the arm angle of the humanoid with/without τ_8 . As τ_8 is inputted, the phase of arm



Fig. 6. Z-Position of free-leg in one step

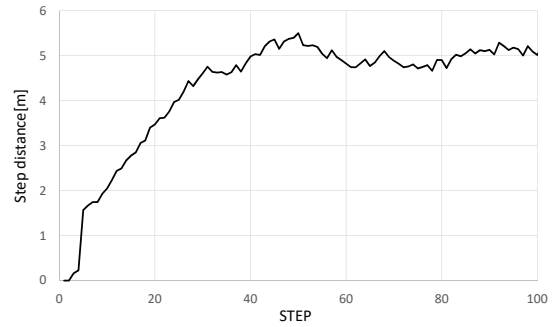


Fig. 7. Slip distance per step up to 100 steps

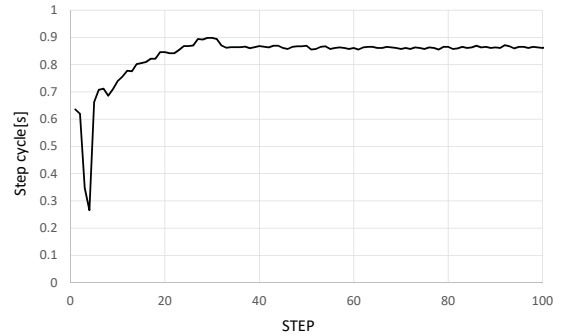


Fig. 8. Step cycle per step up to 100 steps

angle changes from the same to the opposite. It also can be observed that the amplitude of the swing arm has increased. This is thought to be due to the dynamic interference caused by the joint-8. The value of the interference torque obtained by multiplying the element $M_{11,8}$, from the inertia matrix $M(q)$, by the angular acceleration \ddot{q}_8 which is the motion of the yaw angle of the fuselage (joint - 8). The interference torque is shown in Fig.11.

$$\tau_8 = \begin{cases} 30 \sin(2\pi(t - t_e)/2) & (When\ supporting\ foot\ is\ right\ foot) \\ -30 \sin(2\pi(t - t_e)/2) & (When\ supporting\ foot\ is\ left\ foot) \end{cases} \quad (22)$$

5 CONCLUSION

In this paper, was introduced a model of dynamic humanoid considering slip, and it was shown that the motion

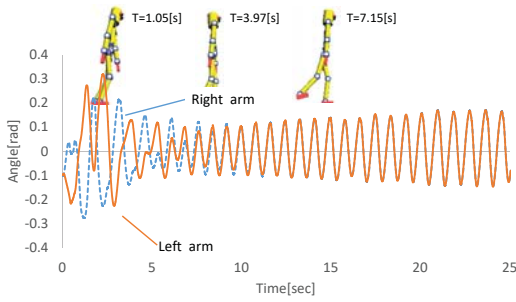


Fig. 9. Arm angle without τ_8

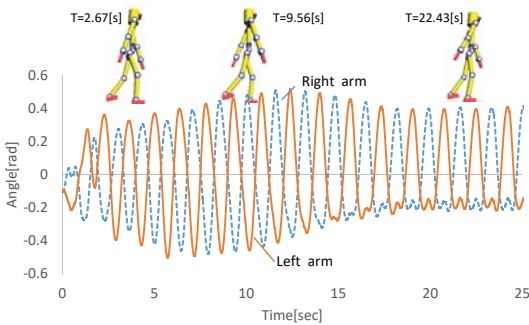


Fig. 10. Arm angle with τ_8

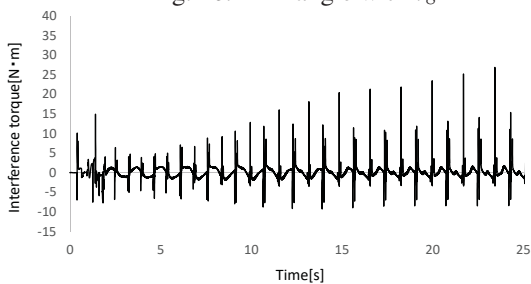


Fig. 11. Interference torque from q_8 to q_{11}

which imitated ice skate was realized by the model. We understand the characteristics of the control using such slips, and we want to make the controller which can cope with the disturbance caused by slips generated during general biped walking.

REFERENCES

- [1] S. Kajita, M. Morisawa, K. Miura, S. Nakaoka, K. Harada, K. Kaneko, F. Kanehiro and K. Yokoi, "Biped Walking Stabilization Based on Linear Inverted Pendulum Tracking," *Proceedings of IEEE/RSJ International Conference on Intelligent Robots and Systems*, pp.4489–4496, 2010.
- [2] H. Dau, C. Chew and A. Poo, "Proposal of Augmented Linear Inverted Pendulum Model for Bipedal Gait Planning," *Proceedings of IEEE/RSJ International Conference on Intelligent Robots and Systems*, pp.172–177, 2010.
- [3] J.H. Park and K.D. Kim, "Biped walking robot using gravity-compensated inverted pendulum mode and computed torque control," *Proceedings of IEEE International Conference on Robotics and Automation*, Vol.4, pp.3528–3593, 1998.
- [4] P.B. Wieber, "Trajectory free linear model predictive control for stable walking in the presence of strong perturbations," *Proceedings of International Conference on Humanoid Robotics*, 2006.
- [5] P.B. Wieber, "Viability and predictive control for safe locomotion," *Proceedings of IEEE/RSJ International Conference on Intelligent Robots and Systems*, 2008.
- [6] A. Herdt, N. Perrin and P.B. Wieber, "Walking without thinking about it," *Proceedings of IEEE/RSJ International Conference on Intelligent Robots and Systems*, pp.190–195, 2010.
- [7] Y. Huang, B. Chen, Q. Wang, K. Wei and L. Wang, "Energetic efficiency and stability of dynamic bipedal walking gaits with different step lengths," *Proceedings of IEEE/RSJ International Conference on Intelligent Robots and Systems*, pp.4077–4082, 2010.
- [8] M. Sobotka and M. Buss, "A Hybrid Mechatronic Tilting Robot: Modeling, Trajectories, and Control," *Proceedings of the 16th IFAC World Congress*, 2005.
- [9] T. Wu, T. Yeh and B. Hsu, "Trajectory Planning of a One-Legged Robot Performing Stable Hop," *Proceedings of IEEE/RSJ International Conference on Intelligent Robots and Systems*, pp.4922–4927, 2010.
- [10] Y. Nakamura and K. Yamane, "Dynamics of Kinematic Chains with Discontinuous Changes of Constraints—Application to Human Figures that Move in Contact with the Environments—," *Journal of RSJ*, Vol.18, No.3, pp.435–443, 2000 (in Japanese).
- [11] J.Nishiguchi, M.Minami, A.Yanou, "Iterative calculation method for constraint motion by extended Newton-Euler method and application for forward dynamics," *Transactions of the JSME*, Vol.80, No.815, 2014.
- [12] T. Feng, J. Nishiguchi, X. Li, M. Minami, A. Yanou and T. Matsuno, "Dynamical Analyses of Humanoid's Walking by using Extended Newton-Euler Method", *20st International Symposium on Artificial Life and Robotics (AROB 20st)*, 2015.
- [13] M. Kouchi, M. Mochimaru, H. Iwasawa and S. Mitani, "Anthropometric database for Japanese Population 1997-98," *Japanese Industrial Standards Center (AIST, MITI)*, 2000.
- [14] T. Maeba, M. Minami, A. Yanou and J. Nishiguchi: "Dynamical Analyses of Humanoid's Walking by Visual Lifting Stabilization Based on Event-driven State Transition", *2012 IEEE/ASME Int. Conf. on Advanced Intelligent Mechatronics Proc.*, pp.7-14, 2012.